Coherent spin dynamics in the nonuniform ferromagnetic InGaAs/GaAs/δ-Mn structures

© S.V. Zaitsev[1], V.V. Dremov[2], V.S. Stolyarov[2]

[1] Osipyan Institute of Solid State Physics, Russian Academy of Sciences,
142432 Chernogolovka, Moscow Oblast, Russia
[2] Center for Photonics and 2D Materials, Moscow Institute of Physics and Technology,
141700 Dolgoprudnyi, Russia

E-mail: szaitsev@issp.ac.ru

Received January 20, 2024
Revised February 26, 2024
Accepted February 29, 2024

A detailed study of the coherent spin dynamics of photoexcited carriers in a heterostructure with an InGaAs/GaAs quantum well and a δ-Mn-layer separated from the quantum well by a $3-10$ nm-thick GaAs spacer indicates its strong non-uniformity in the plane and mesoscopic separation to the regions of carrier localization. Mesoscopic separation with a characteristic scale of $\sim 100-200$ nm is also observed using magnetic force microscopy below the Curie temperature of the δ-Mn-layer.

Keywords: coherent spin dynamics, quantum well InGaAs/GaAs, ferromagnetic δ-Mn-layer, mesoscopic separation, fluctuation potential.

DOI: 10.61011/SC.2024.01.58118.5926

1. Introduction

Control over the spin polarization of carriers in semiconductor systems has become the subject of applied research following the discovery of a dilute magnetic semiconductor (Ga, Mn)As with a record Curie temperature $T_C \sim 170$ K of the ferromagnetic (FM) transition in epilayers [1]. Studies into two-dimensional (2D) semiconductor heterostructures with an FM layer and a quantum well (QW) separated by a tunnel-thin layer (spacer) with thickness $d_S \sim 3-10$ nm are currently underway [2,3]. This design provides an opportunity to control the spin polarization in a QW via the adjacent magnetic semiconductor [4] and retains fine transport and optical properties of a QW. The fact is that interband photoluminescence (PL) is quenched almost completely in FM III$-$Mn$-$V semiconductors by defects (interstitial Mn and various other defects) [1]. Therefore, an FM layer and a QW need to be separated spatially to obtain a sufficiently high PL quantum yield. The influence of an ultrathin FM Mn layer (δ-Mn-layer) on the spin state of carriers in InGaAs/GaAs QWs was examined experimentally in such structures at $d_S = 5-10$ nm: the degree of circular PL polarization was as high as $P_C \sim 10-30\%$ in weak magnetic field $B \sim 0.1-2$ T [5,6]. The model of static exchange $p-d$ interaction of holes in a QW with magnetic impurity spins in a tunnel-close FM layer has long been the universally accepted one for heterostructures with FM layers [1,4]. Stationary (i.e., time-independent) equilibrium spin polarization of carriers in a QW is achieved in this model; therefore, circular polarization of PL from a QW should also be stationary. However, experiments with pulsed excitation provided data indicative of an alternative (dynamic) polarization mechanism with $P_C(t)$ increasing almost linearly with time within a luminescence pulse [6]. The mechanism of dynamic spin polarization of electrons in a QW due to their spin-dependent trapping by polarized donor states of interstitial Mn within an FM δ-layer was substantiated theoretically in [7]. It was demonstrated later in [2] that two carrier polarization mechanisms operate simultaneously in structures with a thin spacer ($d_S \leq 3$ nm): (i) dynamic spin-dependent trapping by defects in the adjacent Mn δ-layer and (ii) static equilibrium $p-d$ exchange of holes with the same FM δ-Mn-layer. In recent paper [3], these structures with InGaAs/GaAs QWs and an FM δ-Mn-layer were examined via optically detected cyclotron resonance (CR). A behavior unusual for nonmagnetic InGaAs/GaAs structures was reported, and the obtained data were interpreted as the observation of magnetoplasma CR of 2D holes within mesoscopically small QW regions. The separation of FM structures into submicrometer-sized regions with a typical size of ~ 100 nm, which was hinted at by magnetotransport measurements [8], was observed in [3] by magnetic force microscopy. Therefore, the study of spin-dependent phenomena in such nonuniform FM heterostructures is definitely important for current spintronics.

In the present study, the coherent spin dynamics of carriers in InGaAs/GaAs/δ-Mn structures with spacer $d_S = 3-10$ nm between the δ-layer and a QW was examined using the magneto-optical Kerr effect method with a picosecond temporal resolution. A strong dependence of the hole component of the Kerr rotation signal on the external magnetic field and the photoexcitation level was recorded, indicating significant disordering and a large-scale localizing potential for carriers in a QW due to mesoscopic separation of the acceptor δ-layer with a characteristic scale of $\sim 100-200$ nm.

2. Samples and experimental procedure

The Kerr effect was studied with a picosecond temporal resolution in the Voigt geometry (with magnetic field B parallel to the sample surface) in a cryostat with a superconducting magnet in superfluid helium (temperature $T \approx 1.8$ K and $B = 0-3$ T) or in a continuous-flow helium cryostat with an adjustable temperature ($T \geq 7$ K) where field $B = 0-0.7$ T was produced by an external electromagnet. A titanium–sapphire laser with a pulse duration of 150 fs and a frequency of 82 MHz was used for excitation. An acoustooptical filter limited the spectral bandwidth of pulses to ~ 0.5 nm and extended them to ~ 2 ps. A delay line provided an opportunity to perform „pump-probe" measurements with time $t < 3$ ns between pump and probe beams varying with a pitch of ~ 0.2 ps. A photoelastic modulator with a frequency of 50 kHz was used to modulate circular polarization of a pump pulse. A circularly polarized pump pulse produced spin-polarized carriers in the sample within a photoexcitation spot $\sim 100\,\mu$m in diameter. This was detected by measuring the angle of rotation of the polarization plane of a linearly polarized probe beam reflected off the sample. In the continuous-flow cryostat, the time-averaged power density of the probe beam was $P_{\text{test}} \sim 5$ W/cm^2, while the same parameter of the pump beam was adjusted within a wide range of $P_{\text{opt}} = 10-300$ W/cm^2, which is one of the important aspects of the present study. In experiments with the superconducting magnet ($T \approx 1.8$ K), pumping was always set to $P_{\text{opt}} \sim 3$ mW at $P_{\text{test}} \sim 0.5$ mW. The diameter of the probe beam spot on the sample was smaller than the photoexcitation spot, which was adjusted by a different aperture (with visual monitoring with a microscope). A balance photodetector combined with a lock-in detector were used to detect the signal of polarization plane rotation at the modulation frequency. Measurements were performed in the spectrally degenerate mode: the wavelengths of pump and probe beams were equal. The sample holder was designed so as to allow one to adjust the angle between the magnetic field direction and crystallographic axes with an accuracy of $\sim 2°$.

LED structures with InGaAs/GaAs QWs and a δ-Mn-layer were grown using a hybrid epitaxial method [5,8]. The diagram of the structure is shown in the inset in Figure 1, *a*. At the first stage, a buffer *n*-GaAs layer $\sim 0.5\,\mu$m in thickness doped with Si ($\sim 10^{17}$ cm^{-3}) was grown by metalorganic chemical vapor deposition on a *n*-GaAs (001) substrate at a temperature of 600°C. An undoped GaAs layer with a thickness of 3 nm, a $In_xGa_{1-x}As$ QW layer (with a thickness of 10 nm and indium content $x_{\text{In}} = 10\%$), and a GaAs spacer layer $d_S = 2-10$ nm in thickness were grown next in succession. An acceptor δ-Mn-layer ~ 0.3 monolayers in thickness (with layer concentration of manganese $N_{\text{Mn}} \sim 2 \cdot 10^{14}$ cm^{-2}) and a cover GaAs layer 40 nm in thickness were then grown in sequence in the same reactor at a temperature of 450°C by laser sputtering of Mn and GaAs targets. Owing to δ-doping, the QW contains

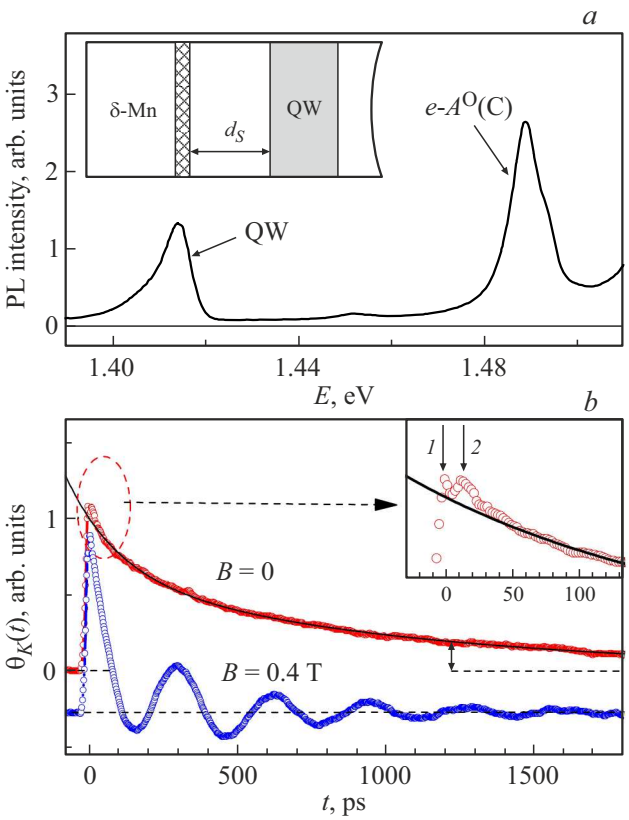

Figure 1. *a* — PL spectrum of the structure with $d_S = 10$ nm at $T = 1.8$ K (the photoexcitation laser has $\lambda \sim 800$ nm). Arrows denote optical transitions in a QW and at neutral carbon acceptors in the GaAs barrier (QW and $e-A^O$(C), respectively). *b* — Kerr signals of polarization plane rotation $\theta_K(t)$ (shifted vertically) at $E_L = 1.414$ eV (≈ 877 nm) in the same structure at $B = 0$ and 0.4 T ($T = 1.8$ K). The zero signal level is represented by dashed lines. The initial stage of signal relaxation at $B = 0$ is presented in the inset. The solid curve is the result of fitting of experimental data with formula (1) at $t > 40$ ps.

2D hole gas with concentration $p_S \sim 10^{11}-10^{12}$ cm^{-2} and Hall mobility $\mu \sim 500-3000$ cm^2/(V·s) at $T = 5$ K (these values vary with the sample parameters) [8]. The magnetic properties of InGaAs/GaAs/δ-Mn structures have already been examined with a SQUID magnetometer, which verified the ferromagnetism of δ-Mn-layers with Curie temperature $T_C \sim 35-40$ K [9]. Magnetic force microscopy (MFM) studies of the surface and the magnetic flux structure were performed using an AttoCube AttoDry 1000 atomic force microscope (AFM) within the 4–50 K temperature range with an accuracy of ~ 0.1 K in helium atmosphere under pressure $P \sim 0.5$ mbar. Silicon magnetic cantilevers coated with a CoCr layer served as probes. The surface topography was examined in the semi-contact mode, and the magnetic flux structure was analyzed in the FMF mode with feedback switched off at a height of ~ 110 nm above the sample surface. The phase shift of magnetic cantilever oscillations was measured to obtain MFM images.

3. Results and discussion

The PL spectrum below the interband transition in a GaAs barrier (~ 1.51 eV) is presented in Figure 1, *a*. In addition to the QW line with a maximum at $E_{QW} = 1.414$ eV, the spectrum features a strong $e-A^{O}(C)$ optical transition line with an energy of ~ 1.49 eV that corresponds to recombination of a free electron and a hole trapped at a neutral carbon acceptor in the GaAs barrier. This is attributable to the use of metalorganic compounds in epitaxy. Kerr signals $\theta_K(t)$ of polarization plane rotation in magnetic fields $B = 0$ and 0.4 T at $T = 1.8$ K measured for the structure with $d_S = 10$ nm in „pump-probe" experiments are shown in Figure 1, *b*. Measurements were performed at laser energy $E_L = E_{QW}$. It is important to note that the $\theta_K(E_L)$ signal amplitude reaches its maximum at $E_L = E_{QW}$; therefore, in contrast to the single-beam Kerr effect [10], the spin dynamics of carriers excited exactly in a QW is examined in this experiment. The $\theta_K(t)$ signal dynamics is characterized well by a sum of two exponential functions with one of them featuring an oscillatory factor with frequency Ω_L:

$$\theta_K(t) = \theta_e \exp(-t/\tau_e)\cos(\Omega_L t + \varphi) + \theta_h \exp(-t/\tau_h). \quad (1)$$

Here, τ_h and τ_e are the times of spin dephasing of holes and electrons, respectively; Ω_L is the Larmor precession frequency that depends linearly on magnetic field as $\hbar\Omega_L(B) = |g|\mu_B B$, where coefficient g is the Landé g-factor in the formula for carrier energy level splitting $\Delta E(B)$ in a magnetic field and $\mu_B \approx 0.058$ meV/T is the Bohr magneton.

Larmor frequency $\Omega_L(B)$ of $\theta_K(t)$ beats obtained by fitting of experimental $\theta_K(t)$ curves depends linearly on B (Figure 2, *a*), allowing one to determine the absolute value of g-factor: $|g| = 0.53 \pm 0.01$. Note that this method provides only the absolute value of g-factor. In the examined Voigt geometry (magnetic field in QW plane), spin splitting $\Delta E_e(B)$ in the InGaAs/GaAs QW conduction band is significantly greater than hole splitting $\Delta E_h(B)$, and the g-factor of an electron (g_e) is at least an order of magnitude higher than the hole g-factor (g_h) [10]. This allows us to identify the determined value as an electron one $|g_e| = 0.53$, which is close to the results from [11]. The second exponential term $\theta_h(t) = \theta_h \exp(-t/\tau_h)$ in formula (1) needed for fitting of experimental curves characterizes the contribution of photoexcited holes localized at QW potential fluctuations after fast relaxation in energy. Since hole spin dephasing times τ_h are shorter than electron ones (τ_e) [10,11], hole contribution $\theta_h(t)$ decays faster and experimentally observed quantum beats involve spin states of electrons, which is exactly what is characterized by the oscillatory term in formula (1). In addition to oscillatory electron component $\theta_e(t)$ and exponentially damped hole component $\theta_h(t)$, Kerr signal $\theta_K(t)$ features two processes (highlighted in the inset of Figure 1, *b*) at the initial stage of relaxation (~ 20 ps) at low $T = 1.8$ K. Sharp peak *1* near $t = 0$

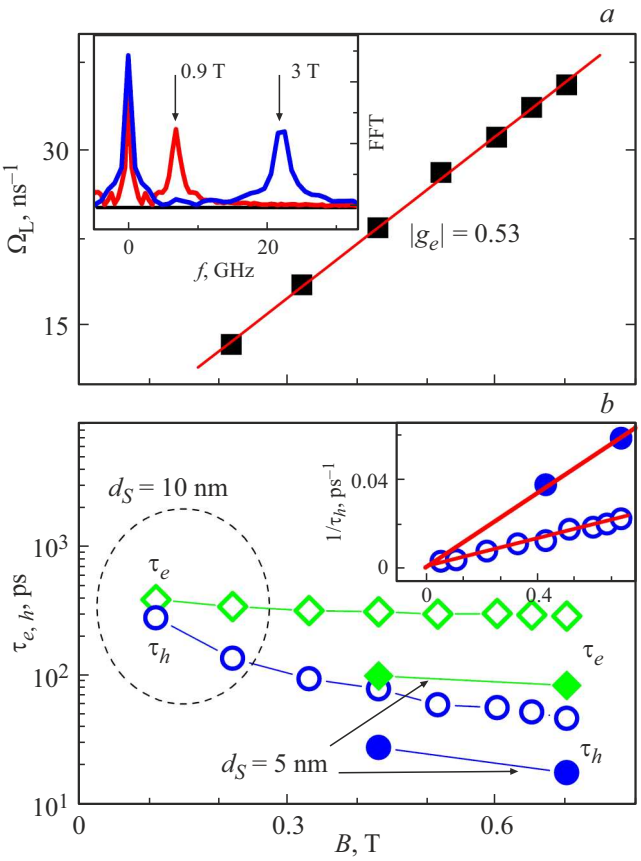

Figure 2. *a* — Magnetic-field dependence of Larmor precession frequency $\Omega_L(B)$ in the structure with $d_S = 10$ nm at $T = 8$ K obtained by fitting with formula (1). The results of fast Fourier analysis of signal $\theta_K(t)$ for $B = 0.9$ and 3.0 T at $T = 1.8$ K are shown in the inset. *b* — Magnetic-field dependences of fitting times $\tau_e(B)$ and $\tau_h(B)$ at $T = 8$ K. The fitting error does not exceed the size of a symbol. Filled and open symbols corresponds to $d_S = 5$ nm and $d_S = 10$ nm, respectively. Inverse hole times $\tau_h^{-1}(B)$ are shown in the inset. Straight lines represent the results of fitting.

corresponds to a coherent artifact [10] produced in temporal overlapping of probe and pump beams and has a width on the order of a doubled laser pulse (~ 4 ps). Peak *2* is associated with spin relaxation of relaxing photoexcited holes that have significantly shorter characteristic times than electrons or holes that have already relaxed and became localized [10]. Fast spin relaxation of photoexcited holes with a characteristic time of ~ 20 ps has also been observed in the study of optical orientation in such structures [6].

In its general form, hole contribution $\theta_h(t)$ to Kerr rotation signal $\theta_K(t)$ should, just as the electron contribution, be characterized by an exponentially damped sinusoid [10]. In a complicated case with several damped oscillation components present, fast Fourier analysis (FFA) provides a more complete representation of the frequency spectrum. Examples of application of FFA to $\theta_K(t)$ for $B = 0.9$ and 3.0 T at $T = 1.8$ K are shown in the inset

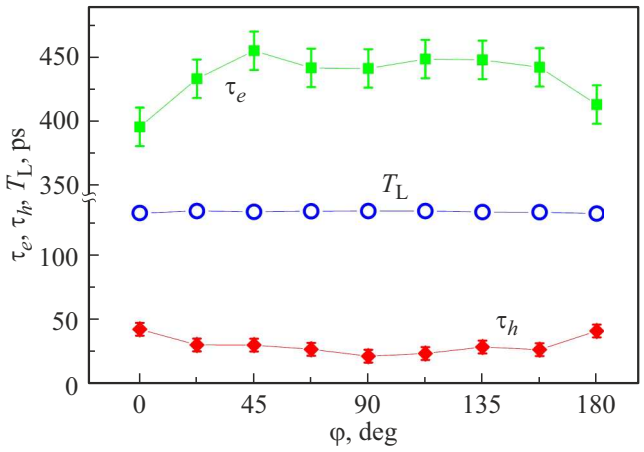

Figure 3. Spin dephasing times and period of Larmor electron oscillations T_L as functions of angle φ between **B** and axis [110] (Voigt geometry) in the structure with $d_S = 10$ nm at $B = 1$ T and $T = 1.8$ K.

of Figure 2, *a*. A sharp peak shifting linearly with magnetic field (frequency $f = \Omega_L/2\pi \approx 22.0$ GHz at $B = 3$ T) corresponds to electron oscillations and agrees with the results of fitting of Larmor electron frequency $\Omega_{L,e}$ with formula (1). At the same time, holes may produce a contribution to the peak at $f \sim 0$, which grows wider with increasing magnetic field, in the FFA spectrum. Larmor hole frequency $\hbar\Omega_{L,h} = \mu_B|g_h^{xy}|B$ may be estimated based on the FWHM of this peak as ~ 2 GHz at $B = 3$ T. This also provides an opportunity to estimate the g-factor of holes: $|g_h^{xy}| \leq 0.05$. Note that owing to the choice of Voigt geometry [10], the carrier g-factor component (g_e^{xy} or g_h^{xy}) in the xy QW plane is measured. In view of the smallness of $|g_h^{xy}|$, the period of Larmor hole oscillations is $T_{L,h} = 2\pi/\Omega_{L,h} \geq 2.5$ ns at $B = 0.4$ T, being significantly longer than decay time $\tau_h \sim 0.15$ ns of the hole component at $T = 1.8$ K. This is the reason why Larmor hole oscillations are not observed experimentally.

Spin relaxation time τ_e and the g-factor of electrons in doped *n*-type GaAs/AlGaAs QWs depend non only on the concentration of two-dimensional electrons in a QW, but, owing to the asymmetry of 2D structures, also on the orientation of the magnetic field relative to crystallographic directions (see [12] and references therein). Kerr curves $\theta_K(t)$ for various angles φ between magnetic field **B** and crystallographic direction [110] falling within the range of $\varphi = 0-180°$ at $B = 1$ T were used to study anisotropy in the structure plane. Figure 3 presents the dependences of period $T_L = 2\pi/\Omega_L$ of Larmor electron oscillations and decay times on angle φ. It is evident that τ_e and τ_h have a considerable anisotropy (difference between values at $\varphi = 0$ and $\varphi = 90°$), which is weaker for electrons ($\sim 13\%$) and stronger for holes ($\sim 50\%$). At the same time, g-factor $g_e \sim 1/T_L$ is, to within a small percentage ($\leq 1\%$), independent of the field orientation. This anisotropy of spin coherence times of carriers, which is more pronounced for holes, is essentially indicative of anisotropy of the localizing fluctuation potential, which is discussed in detail below. Another possible factor leading to anisotropy in the QW plane is the influence of internal stresses in the structure that affect the g-factor and spin relaxation times in different ways: while having almost no effect on g_e, they induce a significant τ_e anisotropy. This examined theoretically and experimentally in [13]. Note that in contrast to the electron anisotropy, the anisotropy of hole times has not been examined in detail yet.

Decay times of Kerr components $\theta_e(t)$ and $\theta_h(t)$ in formula (1) have the following constituent parts [10]:

$$1/\tau_{e(h)} = 1/\tau_{e(h)}^S + 1/T_2^{inh} + 1/\tau. \qquad (2)$$

Here, $\tau_{e(h)}^S$ is the electron (hole) spin relaxation time and $T_2^{inh} = \hbar/(\Delta g_{e(h)}\mu_B B)$ is the dephasing time of spin coherence in a carrier ensemble due to QW nonuniformity, where $\Delta g_{e(h)}^{xy}$ is the spread of electron (hole) g-factor values and τ is the carrier lifetime including radiative and non-radiative channels. For example, $\tau \sim 400$ ps in the structure with $d_S = 10$ nm and $\tau \sim 30-70$ ps for $d_S = 5$ nm at $T = 1.8$ K (depends also on optical pumping), while the spin relaxation of electrons proceeds much slower: $\tau_e^S \sim 10$ ns ($d_S = 10$ nm) and $\tau_e^S \sim 1$ ns ($d_S = 5$ nm) [6]. When τ is the shortest time (in structures with a narrow spacer $d_S \leq 3$ nm where $\tau < 15$ ps and Larmor oscillations are not observed), it specifies the Kerr signal decay time. Therefore, the structure with $d_S = 10$ nm, which has the highest τ, was chosen for detailed studies into coherent carrier spin dynamics. According to formula (2), the primary magnetic-field contribution to spin coherence dephasing should be produced by a term linear in field associated with nonuniformity Δg of the carrier g-factor. Figure 2, *b* shows times $\tau_e(B)$ and $\tau_h(B)$ in structures with $d_S = 5$ nm and 10 nm in fields $B = 0.1-0.7$ T at $T = 8$ K. It is evident that hole time $\tau_h(B)$ undergoes the greatest change (an order-of-magnitude reduction with an increase in the field intensity) at $B > 0.1$ T, while $\tau_e(B)$ decreases only be a factor of ~ 2. The experimentally observed liner dependence of inverse time $\tau_h^{-1}(B)$ (see the inset in Figure 2, *b*) provides an opportunity to estimate spread $\Delta g_h \sim 0.22$ of the hole g-factor. A large Δg_h value, which is significantly greater than the FFA estimate of the g-factor ($|g_h^{xy}| \leq 0.05$), is indicative of strong disordering of the examined structures. It was demonstrated experimentally and theoretically in [14] that the localization of holes induced by disordering of the potential does indeed exert a determining influence on the contribution to $\tau_h^{-1}(B)$ linear in field in doped *n*-type GaAs/AlGaAs QWs. At the same time, the electron g-factor nonuniformity determined from a linear $\tau_e^{-1}(B)$ section is significantly lower: $\Delta g_e \sim 0.0085$. This is indicative of a weak influence of the localizing potential on electrons. The difference in behavior of electrons and holes is attributable to the complex nature of the energy spectrum of the valence band, which induces mixing of states of light and heavy holes and a strong anisotropy of the hole g-factor

in QWs [15]. Times τ_h in the structure with $d_S = 5$ nm are significantly shorter (Figure 2, *b*), while the *g*-factor spread is greater: $\Delta g_h \sim 0.5$. Thus, as the spacer grows thinner, disordering and hole localization at potential fluctuations in a QW become stronger.

Thus, it is the presence of a tunnel-close acceptor δ-layer that induces significant disordering in the examined structures. Note that strong disordering, which is also evidenced by a large FWHM value of PL lines (> 10 meV, Figure 1, *a*), is a common feature of various structures containing FM (Ga,Mn)As layers [1]. Owing to strong diffusion of Mn atoms into GaAs [1], a thin ($\sim 2-3$ nm) FM layer of the $Ga_{1-x}Mn_xAs$ solid solution with a high manganese concentration ($x = 2-6$ at%) actually forms instead of a growing δ-Mn-layer. This is verified by the results of small-angle X-ray diffraction studies [8]. In addition, FM *p*-type semiconductor $Ga_{1-x}Mn_xAs$ contains not only acceptor Mn_{Ga} manganese atoms, but also a high concentration of defects, such as interstitial Mn_I and antisite As_{Ga} [1]. Since these defects act as deep donors and centers of strong non-radiative recombination, the PL intensity in such structures is significantly lower than in those without Mn [5–7]. Specifically, the QW line is an order of magnitude weaker even with a $d_S = 10$ nm spacer, indicating that the δ-Mn-layer produces a dominant contribution to non-radiative recombination. The fact is that the limit of equilibrium solubility of Mn in GaAs is very low (~ 0.1 at%); at high concentrations, „excess“ Mn occupies interstitial sites Mn_I in the GaAs matrix or precipitates in the form of clusters of MnAs ($T_C = 315$ K) and Mn_yGa_{1-y} ($T_C \sim 600$ K) FM phases [1]. This is the reason why non-equilibrium low-temperature methods are used (as was done in the present case) to grow structures with $Ga_{1-x}Mn_xAs$ layers [4,7,8]. A strong mutual donor (Mn_I or As_{Ga}) and acceptor (Mn_{Ga}) compensation is a characteristic feature of δ-Mn-layers grown this way [8]. Since the concentration of Mn atoms in the δ-layer ($N_{Mn} \geq 6 \cdot 10^{13}$ cm^{-2}) is significantly higher than the hole concentration in QWs ($p_S < 2 \cdot 10^{12}$ cm^{-2}), holes cannot screen random fluctuations of the distribution of charged defects completely. This leads to the emergence of a strong long-range Coulomb fluctuation potential (FP) for carriers in a QW [8]. The parameters of this FP and its effect on conductivity and the anomalous Hall effect typical of FM structures were thoroughly examined experimentally and modeled in [8,16]. Specifically, length R of non-screened potential fluctuations falls within the range from minimum $R_{min} \sim d_S$ to maximum $R_{max} \approx N_{Mn}^{1/2}/p_S$; at $R > R_{max}$, fluctuations of the distribution of charged defects are already screened efficiently by holes in a QW. At typical values of $N_{Mn} \sim 6-20 \cdot 10^{13}$ cm^{-2} and $p_S \sim 3 \cdot 10^{11}$ cm^{-2}, we find an estimate $R_{max} \sim 200$ nm. FP amplitude γ is estimated at $\gamma \geq 10$ meV [8], which exceeds the Fermi energy at typical hole concentrations. Note that the considered model of structures with a δ-Mn-layer is distinct in assuming strong spatial variations of the Mn concentration both in the δ-Mn-layer itself and in its neighboring spacer and cover layers, which should also lead to significant nonuniformity of their crystalline and magnetic structures [8,17]. It is assumed that a quasi-2D magnetic phase in the form of individual submicrometer FM regions („islands“ of the $Ga_{1-x}Mn_xAs$ solid solution with a high Mn concentration [17]) forms near the δ-layer. It is the nonuniformity of distribution of Mn atoms that induces separation of the δ-Mn-layer into FM and paramagnetic „islands“ and leads to the emergence of a large-scale Coulomb FP, which correlates with the separated δ-Mn-layer due to the specifics of ferromagnetism in semiconductor $Ga_{1-x}Mn_xAs$ wherein carriers (holes) also act as mediators of the exchange coupling of Mn ions, in the QW plane [1]. Within this model, holes in a QW are localized at FP potential wells near such FM „islands“ [8].

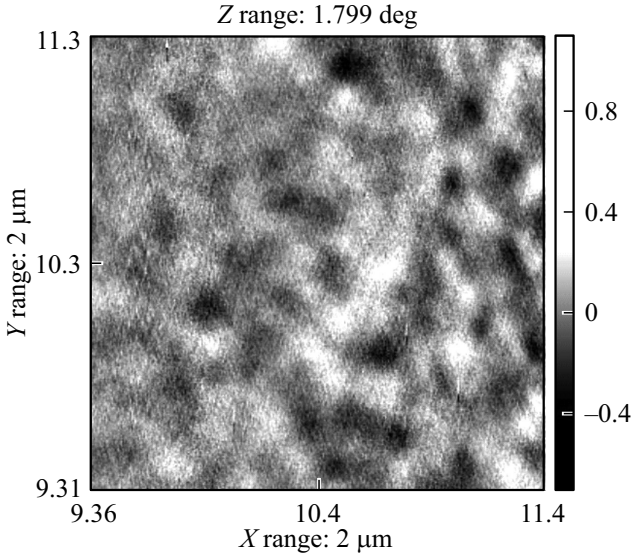

Figure 4. Magnetic flux structure in the sample with $d_S = 10$ nm in the MFM mode. The region size is $2 \times 2\,\mu$m, and full contrast of an oscillation phase of the magnetic cantilever is 1.8°. Field $B = 0.15$ T is directed perpendicularly to the QW plane; $T = 10$ K.

The separation of the δ-Mn-layer into submicrometer FM regions with a characteristic scale of ~ 100 nm, which was conjectured in [8,16,17] based on the results of analysis of transport and magnetic data, is observed directly by MFM [3]. The results of MFM studies for the sample with $d_S = 10$ nm at $T = 10$ K are presented in Figure 4. It is evident that the characteristic scale of nonuniformities in the QW plane for an oscillation phase of the magnetic cantilever is $\sim 100-200$ nm. The observed pattern of magnetic nonuniformity of the FM δ-Mn-layer and its separation into specific „islands“ (domains) is typical of the entire sample and vanishes above its Curie temperature $T_C \sim 35$ K. It should be stressed that the distinct design of a structure with a high-concentration acceptor δ-Mn-layer is exactly the factor that induces an anomalously strong fluctuation Coulomb potential for carriers in a QW.

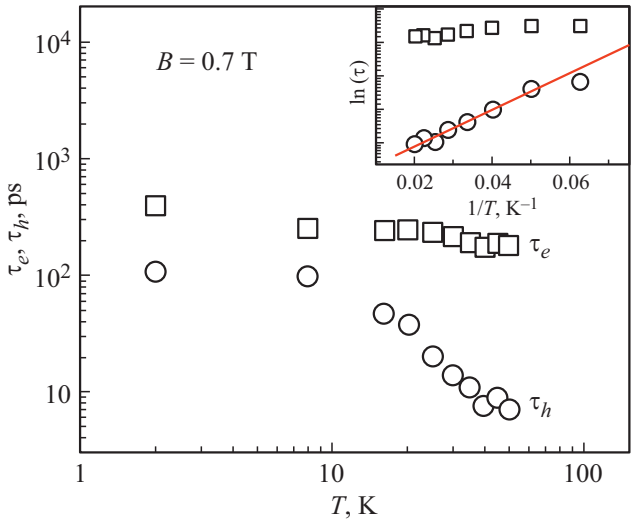

Figure 5. Dependences of times τ_e and τ_h on temperature in the sample with $d_S = 10$ nm. $B = 0.7$ T; $P_{\text{opt}} = 100$ W/cm^2. Dependences of times $\tau_{e,h}(T)$ on reciprocal temperature are shown in the inset. The straight line is the result of linear fitting for holes with dependence $\tau_h(T) = \tau_0 \exp(E_a/T)$.

Under the conditions of strong disordering that is typical of the examined structures, the examination of dependences of such parameters of Kerr rotation $\theta_K(t)$ as spin coherence times τ_e and τ_h and amplitudes of electron and hole components θ_e and θ_h on temperature and optical pumping power provides important insights into the nature of this disorder [18]. For example, the spin dephasing time of photoexcited holes determined in [19] ($\tau_h \sim 110$ ps at $B = 1$ T and $T = 1.6$ K) decreases rapidly with increasing temperature, becoming two times shorter at $T = 6$ K. This is indicative of importance of hole localization, which suppresses spin relaxation of free carriers, at potential fluctuations [10]. The localization energy was estimated at $E_a \sim 0.5$ meV [19], which is comparable to the thermal energy at $T = 6$ K. Dependences $\tau_e(T)$ and $\tau_h(T)$ in the structure with $d_S = 10$ nm are shown in Figure 5. The also suggest that hole localization plays a significant part in the examined structures; notably, E_a increases substantially. It can be seen that $\tau_h(T)$ for holes drops sharply at temperatures greater than $T \sim 10$ K (by more than an order of magnitude within the 10–50 K range), while $\tau_e(T)$ for electrons decreases by a factor of less than 2. Activation dependence $\tau_h(T) = \tau_0 \exp(E_a/T)$ (see the inset in Figure 5) may be used to approximate the hole time within this section. The hole localization energy is estimated at $E_a = 4.8 \pm 0.3$ meV, which is significantly higher than the corresponding value in non-magnetic structures [19] and is close in order of magnitude to estimates of the fluctuation potential amplitude ($\gamma \sim 10$ meV) from [8,16].

The dependences on pumping at $T = 8$ K and $B = 0.7$ T are shown in Figure 6. Measurements were carried out at a low probe beam power density $P_{\text{test}} \sim 5$ W/cm^2. Signal $\theta_K(t)$ was fitted with formula (1) within the $t > 50$ ps section (following the termination of fast initial relaxation at ~ 20 ps). It follows from Figure 6, *a* that electron component $\theta_e(P_{\text{opt}})$ is almost linear within the entire P_{opt} range, while $\theta_h(P_{\text{opt}})$ reaches saturation at pump power densities above $P_0 \sim 50$ W/cm^2. If we assume that the absorption coefficient in an InGaAs/GaAs QW is $\sim 5 \cdot 10^4$ cm^{-1} [10], the observed θ_h saturation corresponds to concentration $n_0 = p_0 \sim 10^{11}$ cm^{-2} of electron–hole pairs excited resonantly in a QW by a single laser pulse. This is comparable to concentration $p_S \sim 10^{11}$ cm^{-2} of resident holes typical of structures with a δ-Mn-layer [8] and may potentially point at the trion mechanism of polarization of resident carriers in a QW (see [19,20]). It should be stressed that the observed dependences on pumping cannot be attributed to thermal lattice heating, since both τ_e and τ_h should fall in this case; instead, $\tau_h(P_{\text{opt}})$ actually increases with P_{opt} (Figure 6, *b*).

The issue of origin of electron and hole contributions to Kerr rotation signal $\theta_K(t)$ appears to be intriguing and important when set in comparison with earlier-examined cases of pulsed photoexcitation of coherent spin precession of resident carriers in doped structures: electrons in *n*-type

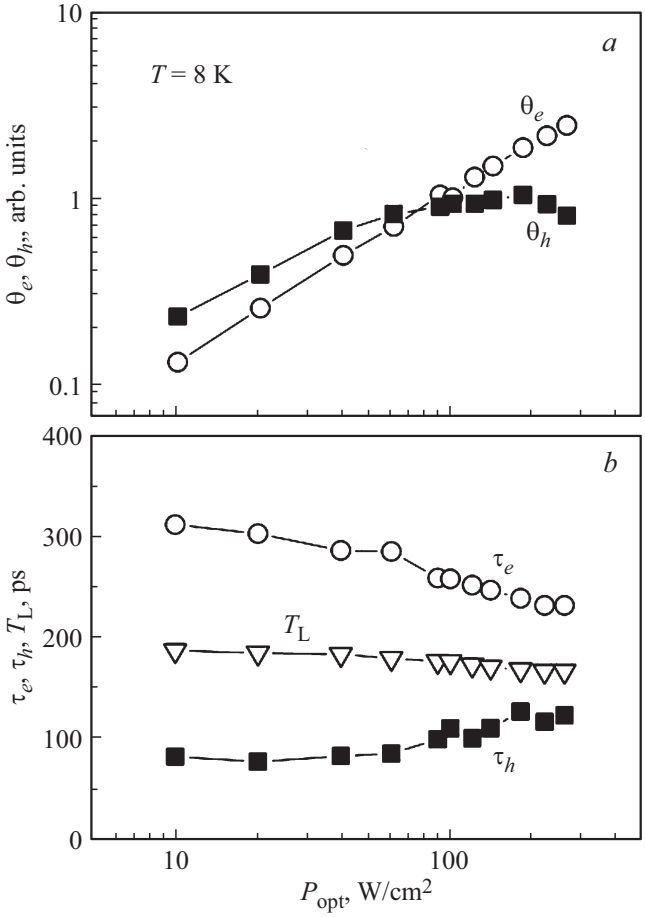

Figure 6. *a* — Dependences of amplitudes θ_e and θ_h of electron and hole Kerr rotation components on average optical pumping power density P_{opt} at $B = 0.7$ T and $T = 8$ K in the sample with $d_S = 10$ nm. *b* — Dependences of spin coherence times τ_e, τ_h and Larmor period T_L on P_{opt}.

QWs [18] and holes in p-type QWs [19–21]. It was found in [19–21] that signal $\theta_K(t)$ has a duration of several nanoseconds, which exceeds significantly the recombination lifetime (~ 100 ps at $T \sim 1.5$ K) and corresponds to coherent precession of resident holes in a QW induced by photoexcited carriers. A combined model of spin and recombination carrier dynamics was considered in [21] as a means to explain the effect of long-lived coherent precession of resident holes in high-quality GaAs/AlGaAs QWs with a high mobility $\mu > 10^5$ cm^2/(V·s) at $T = 1.3$ K. Interestingly, long-lived component $\theta_h(t)$ from resident holes in a QW should turn to zero at $B = 0$ in this model after recombination of photoexcited carriers. This is exactly what was observed experimentally [21]. The trion model of polarization of resident holes in a QW [19,20] turned out to be more fitting for GaAs/AlGaAs QWs with a lower hole mobility ($\mu \sim 10^4 - 10^5$ cm^2/(V·s), $p_S \sim 10^{11}$ cm^{-2}), which is closer to the case examined here. Kerr signal duration t_{max} in these studies was also significantly longer than the carrier lifetime (~ 100 ps at $T \sim 1.6$ K) in all magnetic fields: $t_{max} > 3$ ns, which corresponds to coherent precession of resident holes. In addition, it was observed in [19,20] that the long-lived signal component from resident holes in a QW has a negative sign (opposite to the electron contribution) at $B = 0$. This is in line with exactly the trion model. In the studied structures, the electron and hole components of $\theta_K(t)$ have the same sign within the entire range of magnetic fields, and the Kerr signal duration at $T = 8$ K is limited to $t_{max} \sim 1$ ns $\sim 3\tau$ [6], where $\tau \sim 0.4$ ns is the carrier lifetime, This contradicts the trion scenario of photoexcitation of coherent spin precession. Note that t_{max} increases to ~ 3 ns at $T = 1.8$ K (the time window in Figure 1, b is limited). Therefore, the possibility of long-lived coherent precession of resident holes at $T < 1.8$ K cannot be ruled out entirely. This issue warrants further study at low and ultralow temperatures $T \leq 1$ K (similar to the one performed in [11]).

Thus, coherent spin dynamics of carriers in the examined structures with an acceptor FM δ-Mn-layer of a high density differs significantly from the one in doped QWs examined to date, and the trion scenario proposed in [19,20] is ill-suited for these structures. We believe that a different explanation for the experimentally observed saturation of hole component θ_h is valid: the obtained estimate corresponds to the density of defects and other localization centers (N_{loc}) at which photoexctied holes in a QW localize at low temperatures. A strong nonuniformity of the g-factor of holes supports this assumption. Another supporting factor is the result of detailed measurements of transport properties of the studied FM heterostructures [8]. Having observed quantum effects, which are typical of high-quality two-dimensional objects, coupled with activation conductivity and a giant negative magnetoresistance, which is attributable to magnetic disordering, the authors of [8] concluded that these phenomena are indicative of mesoscopic separation of structures with a δ-Mn-layer. The separation of a QW into regions of a high quality and mobility containing degenerate 2D hole gas was suggested. It follows from the analysis of transport data that the characteristic size of such regions is $D_m \sim 100$ nm and the free path length of holes is $l \sim 20$ nm; the regions themselves are separated by thin non-conducting (dielectric) layers [8]. If one estimates the density of localization centers N_{loc} at $N_{loc} \sim 1/D_m^2 \sim 10^{10}$ cm^{-2}, the estimated concentration of photoexcited carriers $p_0 \sim 10^{11}$ cm^{-2} at which θ_h reaches saturation will be just an order of magnitude higher. Note that electrophysical characteristics may vary substantially from one structure to the other [8], making it more difficult to perform such a comparison. The growth of P_{opt} in experiments first leads to filling of hole states in a QW lying deeper in energy, which are localized stronger and feature a more pronounced dispersion of the g-factor that is tied to the characteristics of a specific localized state [15]. A further increase in P_{opt} results in successive filling of less localized hole states with a less pronounced g-factor dispersion. This interpretation is supported by the fact that $\tau_h(P_{opt})$ starts growing at the same $P_{opt} \sim 50$ W/cm^2 (Figure 6, b) as the one corresponding to saturation of the θ_h amplitude. This is illustrative of weakening of the Δg_h dispersion contribution in formula (2). At the same time, spin relaxation time τ_h^S (the first term in $T_{2,h}$) for less localized (in the limit case, free) holes should then shorten as in the case of electrons, which feature insignificant localization and demonstrate $\tau_e(P_{opt})$ reduction that starts at minimum P_{opt} (Figure 6, b). Apparently, the limit of quasi-free holes is not reached in experiments and a complex pattern of overlapping competing contributions, which are manifested differently for electrons and holes, is observed. Note that similar hole times $\tau_h \sim 100$ ps were reported for InP/(Ga, In)P quantum dots with weak confinement [22].

4. Conclusion

We note in conclusion that the obtained results confirm the presence of lateral separation in QWs, which was hinted at earlier by magnetotransport measurements [8], and suggest that a ferromagnetic acceptor high-concentration δ-Mn-layer affects not only the spin polarization of carriers, but also the coherent spin dynamics of holes, which differs considerably from the one for non-magnetic structures. Specifically, coherent precession of resident holes was not observed at temperatures down to $T \sim 2$ K. The saturation of hole component of the Kerr signal at higher pumping levels and an anomalously strong magnetic-field dependence of the hole spin dephasing time are indicative of QW separation into submicrometer regions of carrier localization under a strong fluctuation potential. Mesoscopic separation of the δ-Mn-layer below Curie temperature $T_C \sim 35$ K was revealed by magnetic force microscopy. Carrier spin relaxation times were found to be anisotropic in the QW plane (this effect was stronger for holes), while the electron g-factor was isotropic.

Funding

This study was carried out under the state assignment of the Osipyan Institute of Solid State Physics, Russian Academy of Sciences.

Acknowledgments

The authors wish to thank A.V. Larionov for his help with experiments and M.V. Dorokhin and B.N. Zvonkov for the provided samples.

Conflict of interest

The authors declare that they have no conflict of interest.

References

[1] T. Dietl, H. Ohno. Rev. Mod. Phys., **86**, 187 (2014).
[2] S.V. Zaitsev. Bull. Russ. Acad. Sci.: Phys., **86**, 443 (2022).
[3] S.V. Zaitsev, V.V. Dremov, V.S. Stolyarov. JETP Lett., **116**, 232 (2022).
[4] B.P. Zakharchenya, V.L. Korenev. Phys.-Usp., **48**, 603 (2005).
[5] S.V. Zaitsev, M.V. Dorokhin, A.S. Brichkin, O.V. Vikhrova, Yu.A. Danilov, B.N. Zvonkov, V.D. Kulakovskii. JETP Lett., **90**, 658 (2010).
[6] V.L. Korenev, I.A. Akimov, S.V. Zaitsev, V.F. Sapega, L. Langer, D.R. Yakovlev, Yu.A. Danilov, M. Bayer. Nature Commun., **3**, 959 (2012).
[7] I.V. Rozhansky, K.S. Denisov, N.S. Averkiev, I.A. Akimov, E. Lähderanta. Phys. Rev. B, **92**, 125428 (2015).
[8] M.A. Pankov, B.A. Aronzon, V.V. Rylkov, A.B. Davydov, E.Z. Meilikhov, R.M. Farzetdinova, E.M. Pashaev, M.A. Chuev, I.A. Subbotin, I.A. Likhachev, B.N. Zvonkov, A.V. Lashkul, R. Laiho. J. Exp. Theor. Phys., **109**, 293 (2009).
[9] A.I. Dmitriev, R.B. Morgunov, S.V. Zaitsev. J. Exp. Theor. Phys., **112**, 317 (2011).
[10] D.R. Yakovlev, M. Bayer. In: *Spin Physics in Semiconductors*, ed. by M.I. Dyakonov (Springer, Berlin, 2008) p. 135. https://link.springer.com/chapter/10.1007/978-3-540-78820-1_6
[11] L.V. Fokina, A. Yugova, D.R. Yakovlev, M.M. Glazov, I.A. Akimov, A. Greilich, D. Reuter, A.D. Wieck, M. Bayer. Phys. Rev. B, **81**, 195304 (2010).
[12] A.V. Larionov, A.S. Zhuravlev. JETP Lett., **97**, 137 (2013).
[13] D.J. English, P.G. Lagoudakis, R.T. Harley, P.S. Eldridge, J. Hübner, M. Oestreich. Phys. Rev. B, **84**, 155323 (2011).
[14] X. Marie, T. Amand, P. Le Jeune, M. Paillard, P. Renucci, L.E. Golub, V.D. Dymnikov, E.L. Ivchenko. Phys. Rev. B, **60**, 5811 (1999).
[15] Yu.G. Kusrayev, A.V. Koudinov, I.G. Aksyanov, B.P. Zakharchenya, T. Wojtowicz, G. Karczewski, J. Kossut. Phys. Rev. Lett., **82**, 3176 (1999).
[16] V. Tripathi, K. Dhochak, B.A. Aronzon, V.V. Rylkov, A.B. Davydov, B. Raquet, M. Goiran, K.I. Kugel. Phys. Rev. B, **84**, 075305 (2011).
[17] B.A. Aronzon, A.S. Lagutin, V.V. Ryl'kov, V.V. Tugushev, V.N. Men'shov, A.V. Lashkul, R. Laiho, O.V. Vikhrova, Yu.A. Danilov, B.N. Zvonkov. JETP Lett., **87**, 164 (2008).
[18] E.A. Zhukov, D.R. Yakovlev, M. Bayer, M.M. Glazov, E.L. Ivchenko, G. Karczewski, T. Wojtowicz, J. Kossut. Phys. Rev. B, **76**, 205310 (2007).
[19] M. Syperek, D.R. Yakovlev, A. Greilich, J. Misiewicz, M. Bayer, D. Reuter, A.D. Wieck. Phys. Rev. Lett., **99**, 187401 (2007).
[20] M. Studer, M. Hirmer, D. Schuh, W. Wegscheider, K. Ensslin, G. Salis. Phys. Rev. B, **84**, 085328 (2011).
[21] T. Korn, M. Kugler, M. Griesbeck, R. Schulz, A. Wagner, M. Hirmer, C. Gerl, D. Schuh, W. Wegscheider, C. Schüller. New J. Phys., **12**, 043003 (2010).
[22] M. Syperek, D.R. Yakovlev, I.A. Yugova, J. Misiewicz, M. Jetter, M. Schulz, P. Michler, M. Bayer. Phys. Rev. B, **86**, 125320 (2012).

Translated by D.Safin